Fluorescence decay studies of anisotropic rotations of small molecules

Mary D. Barkley,[a] Andrzej A. Kowalczyk,[b] and Ludwig Brand

Department of Biology and the McCollum-Pratt Institute, The Johns Hopkins University, Baltimore, Maryland 21218

(Received 11 May 1981; accepted 4 June 1981)

The fluorescence decay and the decay of the emission anisotropy of perylene and 9-aminoacridine in glycerol have been investigated at several excitation wavelengths over the temperature range 10 to 40 °C. Under these conditions the fluorescence lifetime of both compounds is essentially constant: about 4.6 ns for perylene and 12.8 ns for 9-aminoacridine. The decay of the fluorescence emission anisotropy could be analyzed in terms of a double exponential function with rotational correlational times independent of excitation wavelength and dependent on temperature. The pre-exponential terms are independent of temperature but do depend on the excitation wavelength as expected from geometrical considerations. The anisotropic character of the rotation of perylene is quite pronounced. Excitation of an absorption dipole perpendicular to the emission dipole gives rise to decay curves for the emission anisotropy showing unusual oscillatory behavior; these are predicted by theory. The rotational dynamics of perylene are consistent with those of a disk with the slipping boundary condition. The ratio of the diffusion coefficients about the axes perpendicular and parallel to the plane of the disk is 10 ± 1, in agreement with previous estimates. The anisotropic character of the rotation of 9-aminoacridine is less striking than that of perylene, but is clearly revealed by measurements at several excitation wavelengths. The rotational dynamics can be interpreted in terms of a hydrodynamic prolate ellipsoid of revolution with a ratio of diffusion coefficients about the major and minor axes of 1.4 ± 0.1 and an axial ratio of about 1.5. Experimental criteria for detecting anisotropic rotations by means of polarized fluorescence are discussed.

I. INTRODUCTION

Anisotropic rotational behavior of small molecules in solution has been observed with the aid of several experimental techniques.[1-4] Such studies yield values for the three principal diffusion coefficients as well as information about the location of the diffusion principal axes, the interaction of the molecule with the solvent, and the structure of the liquid. It has been found that the usual sticking boundary condition[5] of hydrodynamics does not apply to the reorientation of some simple aromatic compounds in viscous fluids.[6] Mantulin and Weber[7] have shown that unsubstituted aromatic hydrocarbons "slip" more rapidly in their own plane than they rotate out of the plane. In contrast, aromatics having substituent groups that hydrogen bond with the solvent undergo isotropic rotational diffusion.

Due to the process of photoselection,[8] fluorescence emission is usually polarized to some extent. Depolarization results from rotational diffusion or energy transfer. The orientational distribution of excited chromophores has an axis of symmetry created by the exciting light.[9] Consequently, in the case of an anisotropic rotator, some rotations do not result in depolarization. According to Perrin's theory[10] the fluorescence depolarization of nonspherical molecules is expected to depend on the wavelength of excitation. This property has been used to detect anisotropic rotations by steady-state fluorescence depolarization.[11-13] Although there are several indicators of anisotropic motions from steady-state measurements, such as curvature of Perrin plots, emission anisotropies at different excitation wavelengths, and lifetime-resolved emission anisotropies, these approaches provide crude estimates of the ratio of the principal diffusion coefficients. Similarly, the tangent defect obtained by differential phase fluorimetry[14] affords a simple test for the existence of anisotropic rotations, but again gives only relative values of the diffusion coefficients. In theory, absolute values of the principal diffusion coefficients for anisotropic rotators can be determined from the time-resolved fluorescence emission anisotropy. However, the full anisotropic rotational diffusion may not be evident in measurements at a given excitation wavelength. Even in cases where anisotropic rotations contribute multiple exponential terms to the decay of the emission anisotropy, the information content of the data obtained at a single wavelength is often not sufficient to resolve all the decay parameters.

In this paper we present a detailed investigation of anisotropic rotations by pulsed nanosecond fluorimetry at several excitation wavelengths. Two fluorophores (perylene and 9-aminoacridine) were selected for study on the basis of their known spectral and rotational properties. Both aromatic compounds have strong $\pi \rightarrow \pi^*$ transitions in the visible and ultraviolet regions, which are positively and negatively polarized. Previous findings[4,7] suggested that these molecules represent extremes of rotational behavior, perylene being a highly anisotropic rotator with the slipping boundary condition and 9-aminoacridine an isotropic rotator with the sticking boundary condition. We determine the decay of the emission anisotropy, exciting absorption dipoles both parallel and perpendicular to the emission dipoles, and analyze the data for a consistent set of decay parameters. The dependence of the decay parameters on temperature and viscosity is also determined. This method enables us to deduce the location of the diffusion principal axes for perylene and 9-aminoacridine and to calculate the principal diffusion coefficients. The dimensions of the rotating ellipsoids are also computed. The results

[a] Present address: Department of Biochemistry, University of Kentucky Medical Center, Lexington, Ky 40536.
[b] Present address: Institute of Physics, N. Copernicus University, 87-100 Torun, Poland.

 0021-9606/81/193581-13$01.00 © 1981 American Institute of Physics

Downloaded 01 May 2008 to 150.131.77.142. Redistribution subject to AIP license or copyright; see http://jcp.aip.org/jcp/copyright.jsp

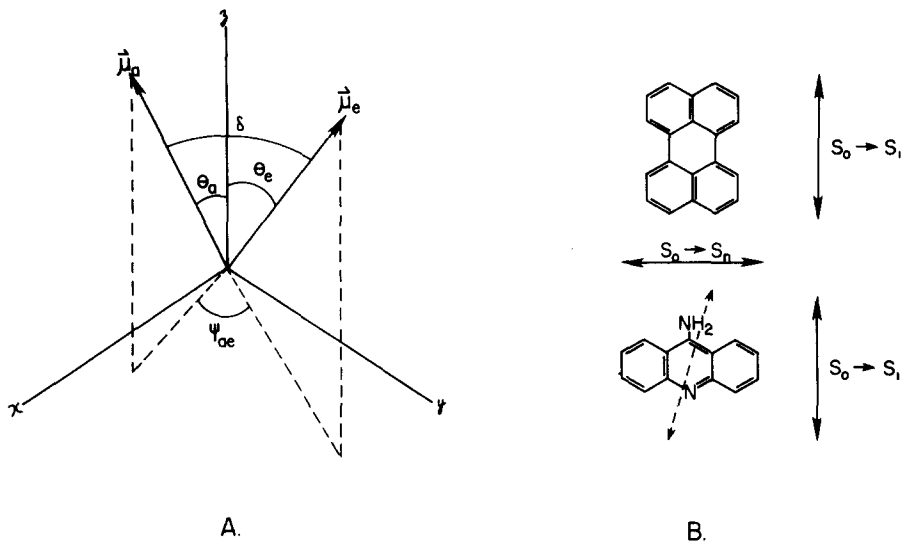

FIG. 1. Transition dipole directions. (A) Diffusion principal axes of ellipsoid of revolution with symmetry axis along z; μ_a: absorption dipole; μ_e: emission dipole; θ_a angle between μ_a and symmetry axis; θ_e: angle between μ_e and symmetry axis; ψ_{ae}: angle between azimuths of μ_a and μ_e; δ: angle between μ_a and μ_e. (B) Absorption dipole directions of perylene (upper) and 9-aminoacridine (lower). $S_0 \rightarrow S_1$ at 430 nm; $S_0 \rightarrow S_n$ at 256 or 260 nm. Broken line shows emission dipole direction at 460 nm for 9-aminoscridine.

demonstrate that nanosecond time-resolved emission anisotropy experiments with excitation of differently oriented absorption oscillators can be used as a sensitive, quantitative technique for studying anisotropic rotational diffusion.

II. THEORY

The fluorescence emission anisotropy for linearly polarized exciting light is defined as

$$r(t)=\frac{I_V(t)-I_H(t)}{I_V(t)+2I_H(t)}\,, \tag{1}$$

where the subscripts V and H denote vertically and horizontally polarized components of the emission intensity $I(t)$, respectively. The decay of the emission anisotropy of a general rigid ellipsoid is described by a sum of five exponential terms[15-17]

$$r(t)=\sum_{i=1}^{5}\beta_i \exp(-t/\phi_i)\,. \tag{2}$$

However, because two pairs of the rotational correlation times ϕ_i are approximately equal, in practical cases no more than three exponentials will be observed.[18] For ellipsoids of revolution the emission anisotropy is also a sum of three exponentials. The pre-exponential terms β_i are simple trigonometric functions of the angles between the transition dipoles and the symmetry axis of the ellipsoid (Fig. 1):

$$\beta_1 = 0.1(3\cos^2\theta_a - 1)(3\cos^2\theta_e - 1)\,, \tag{3a}$$

$$\beta_2 = 0.3\sin^2\theta_a \sin^2\theta_e \cos 2\psi_{ae}\,, \tag{3b}$$

$$\beta_3 = 1.2\sin\theta_a\cos\theta_a\sin\theta_e\cos\theta_e\cos\psi_{ae}\,, \tag{3c}$$

where θ_a and θ_e are the angles made by the absorption and emission dipoles with the symmetry axis, respectively, and ψ_{ae} is the angle between their projections in the plane perpendicular to the symmetry axis. The pre-exponentials should thus depend on the wavelength of excitation. (In the case of a general ellipsoid, they are also dimensionless functions of the principal diffusion coefficients but independent of temperature and viscosity.) The corresponding rotational correlation times are given by

$$\phi_1^{-1} = 6D_\perp\,, \tag{4a}$$

$$\phi_2^{-1} = 2D_\perp + 4D_\parallel\,, \tag{4b}$$

$$\phi_3^{-1} = 5D_\perp + D_\parallel\,, \tag{4c}$$

where $D_\perp$ is the rate of rotation about an axis perpendicular to the symmetry axis, and $D_\parallel$ is the rate of rotation about the symmetry axis.

The principal diffusion coefficients are functions of the size and shape of the rotating fluorophore and of the temperature T and viscosity η of the solvent. The values also depend on the nature of the interaction between the fluid and the surface of the molecule. In the case of Brownian diffusion, the first layer of solvent moves with the solute molecule (sticking boundary conditions) and the rotational motions are strongly damped. The diffusion coefficients for ellipsoids of revolution are[19]

$$D_\perp = \frac{3\rho[(2\rho^2-1)S-\rho]D}{2(\rho^4-1)}\,, \tag{5a}$$

$$D_\parallel = \frac{3\rho(\rho-S)D}{2(\rho^2-1)}\,, \tag{5b}$$

where ρ is the axial ratio, and where $D=kT/6\eta V$ is the diffusion coefficient for a sphere of volume V equal to that of the ellipsoid, k is the Boltzmann constant, and S is given below. For a prolate ellipsoid, $\rho>1$ and

$$S=(\rho^2-1)^{1/2}\ln[\rho+(\rho^2-1)^{1/2}]\,. \tag{6a}$$

For an oblate ellipsoid, $\rho<1$ and

$$S=(1-\rho^2)^{-1/2}\tan^{-1}[(1-\rho^2)^{1/2}/\rho]\,. \tag{6b}$$

With the sticking boundary condition, $D_\parallel > D_\perp$ for a prolate rotator so that $\phi_1>\phi_3>\phi_2$, whereas $D_\perp \gtrsim D_\parallel$ for an oblate rotator, so that the ϕ_i's are approximately equal (maximum difference about 15%).[18] On the other hand, in the case that the fluid does not stick to the surface of the solute molecule (slipping boundary condition), ellipsoids of revolution undergo essentially free diffusion

Downloaded 01 May 2008 to 150.131.77.142. Redistribution subject to AIP license or copyright; see http://jcp.aip.org/jcp/copyright.jsp

(limited only by inertia) about the symmetry axis.[20] Rotations about the other axes must displace some solvent, though, and these are retarded. With the slipping boundary condition, $D_{\parallel}(-\infty) \gg D_{\perp}$ so that $\phi_1 \gg \phi_2 \approx \phi_3 \to 0$ for both prolate and oblate rotators. Although analytical expressions for $D_{\perp}$ are not available, relative values of the frictional coefficients under slipping and sticking boundary conditions have been computed for various axial ratios.[5] The values of $D_{\perp}(\text{slip})/D_{\perp}(\text{stick})$ decrease from infinity for a sphere to almost unity for very elongated prolates or very flattened oblates. Additional models for rotational diffusion include the intermediate case of a partial slipping boundary condition[11] as well as jump diffusion.[4]

Therefore, depending on the orientations of absorption and emission dipoles and on the interaction of fluorophore and solvent, different values of the pre-exponentials and the rotational correlation times will be observed in the decay of the emission anisotropy. Equations (3) and (4) show that if one of the transition dipoles is directed along a diffusion principal axis (i.e., $\beta_3 = 0$), the decay of the emission anisotropy reduces to a double exponential; further reduction to a single exponential occurs if this axis is the symmetry axis of the ellipsoid (i.e., $\beta_2 = \beta_3 = 0$). The decay is obviously monoexponential in the case of an isotropic rotator (i.e., $D_{\perp} = D_{\parallel}$) Thus, excitation at different wavelengths emphasizes different terms in the decay law for the emission anisotropy, providing a sensitive diagnostic of anisotropic rotations.

III. EXPERIMENTAL

Perylene (Gold Label) was obtained from Aldrich and used without purification. 9-aminoacridine was purchased from K&K Laboratories and recrystallized from acetone. The purity was checked by thin layer chromatography using a variety of solvent systems,[22] by reverse phase high pressure liquid chromatography with absorbance and fluorescence detection, and by mass spectrometry. There was no evidence of impurities in either the commercial or recrystallized compound. Molar extinction coefficients $\epsilon(\lambda)$ of 9-aminoacridine were determined in a Cary 118 spectrophotometer using 0.1 and 1 cm cuvettes. 9-aminoacridine crystals were dried *in vacuo* over P_2O_5, and solutions were prepared by weight in the concentration range 2.5×10^{-2} to 7×10^{-6} M. Glycerol (OmniSolv) from Matheson Coleman and Bell was used as solvent. The water content of the glycerol was determined by NMR to be 1.0% (*w/w*). For fluorescence emission anisotropy measurements the perylene concentration was 2×10^{-6} M and the 9-aminoacridine concentration was 1.2×10^{-5} M. The absorbance of these solutions was about 0.1 at the long wavelength absorption maximum.

Steady-state fluorescence measurements were made with a Perkin-Elmer MPF-4 spectrofluorimeter operating in the ratio mode. Steady-state emission anisotropies were measured with a Polaroid ($\lambda_{ex} > 290$ nm) or Polacoat ($\lambda_{ex} < 300$ nm) polarizer in the excitation path and a Polaroid polarizer in the observation path, and calculated from

$$\langle r \rangle = \frac{I_{VV} \cdot G - I_{HV}}{I_{VV} \cdot G + 2I_{HV}} . \tag{7}$$

Here the first and second subscripts refer to the orientation of the excitation and observation polarizers and the factor $G = I_{HH}/I_{VH}$ corrects for partial polarization of the light source and unequal transmission of the excitation train. The error in steady-state emission anisotropies is about ± 0.002.

Nanosecond time-resolved fluorescence experiments were carried out in a single-photon counting fluorimeter constructed in this laboratory and described elsewhere.[23] Samples were excited with a Photochemical Research Associates nanosecond flash lamp operated at a repetition rate of 18 kHz. Decay curves were collected at a low counting rate (about 3% of the repetition rate of the lamp) to avoid errors from multiple photon detection per flash. The lamp was filled with N_2 at slightly greater than 1 atm pressure, and a small flow of gas was established to prevent fogging of the lamp windows; the electrode gap was about 1 mm. For exciation below 300 nm, the lamp was filled with D_2 at about 0.5 atm pressure and the electrode gap increased to 2–3 mm. Under these conditions, the pulse widths were 1.8–2.4 ns (FWHM) and the shapes slightly asymmetric. Excitation wavelengths were selected by interference filters, and emission wavelengths by a Bausch and Lomb 0.5 m grating monochromator (7 nm bandwidth). The following interference filters were used: Corion 4300, 4000, 3800, 3130, 2600, and 2500 and Baird-Atomic 355. The combination of the transmittance of these filters and the spectral profile of the lamps resulted in effective excitation wavelengths λ_{ex} of 430, 404, 381, 358, 317, 260, and 256 nm (10 nm bandwidth). Samples were excited through Glan-Thompson (air-space) polarizers oriented in the vertical and horizontal directions. Fluorescence emission was observed at right angles through a vertically oriented Polaroid ($\lambda_{ex} > 300$ nm) or Glan-Thompson ($\lambda_{ex} < 300$ nm) polarizer. In each experiment, two decay curves $I_{VV}(t)$ and $I_{HV}(t)$ were collected contemporaneously with the excitation pulse profile as described before.[24] Decay proportional to total fluorescence was obtained by excitation through polarizers oriented at 54.7° to the vertical (magic-angle position *M*). The wavelength-dependent shift between excitation and emission curves was determined under the same optical conditions with excitation polarizers in the magic-angle position, using standard compounds having a single fluorescence lifetime. Monoexponential standards were 9-cyanoanthracene and anthracene in ethanol, as well as perylene and 9-aminoacridine in glycerol. Except for experiments at $\lambda_{ex} = 317$ nm, background fluorescence from the glycerol solvent was negligible. To correct for the low background at $\lambda_{ex} = 317$ nm (1%–2% of the total sample emission), blank curves were collected under identical experimental conditions and subtracted from the sample curves.

For each set of data, a sum curve

$$S(t) = I_{VV}(t) \cdot G + 2I_{HV}(t) \tag{8}$$

and a difference curve

$$D(t) = I_{VV}(t) \cdot G - I_{HV}(t) \tag{9}$$

Downloaded 01 May 2008 to 150.131.77.142. Redistribution subject to AIP license or copyright; see http://jcp.aip.org/jcp/copyright.jsp

were constructed. The factor G, which here also corrects for fluctuations in the lamp intensity and unequal transparency of the excitation polarizers, was obtained by normalizing the total number of counts collected in the two decay curves to the average value of the steady-state emission anisotropy

$$G=\frac{(1+2\langle r\rangle)I_{HV}(t)}{(1-\langle r\rangle)I_{VV}(t)}\ , \tag{10}$$

or by determining the number of counts in I_{HH} and I_{HV} over a given time interval. Because of the finite duration of the excitation pulse and response time of the detection system, the observed decay curves are distorted by convolution with these instrumental factors. The true decay (impulse response) was recovered by an iterative convolution procedure using a nonlinear least squares search based on the Marquardt algorithm.[25] The impulse responses of the total fluorescence $s(t)$ and the emission anisotropy $r(t)$ were assumed to be mono- or biexponential functions: $s(t)=\sum_{i=1}^{k}\alpha_i \times\exp(-t/\tau_i)$ and $r(t)=\sum_{i=1}^{k}\beta_i\exp(-t/\phi_i)$ for $k=1, 2$. The decay parameters of the total fluorescence (α_i, τ_i) were obtained by fitting the experimental sum curve $S(t)$ to the impulse response $s(t)$ convolved with the excitation pulse profile. Fluorescence decay parameters were extracted in a similar fashion from the experimental curve $I_{MV}(t)$ collected with the excitation polarizer in the magic-angle position. The decay parameters of the emission anisotropy (β_i, ϕ_i) were obtained by fitting the experimental difference curve $D(t)$ to the convolved $d(t)=r(t)\cdot s(t)$, using the previously determined $s(t)$. The goodness of fit was measured by the magnitude of the reduced chi square χ_r^2 and the quality of fit judged by the shape of the autocorrelation function A of the weighted residuals.[26] In the computation of weighting factors, the noise in the data was assumed to be photon-counting error and therefore Poisson distributed. It should be emphasized that even small systematic errors accumulate with time, whereas counting error decreases with time. In the case of systematic errors the above weighting is not correct, and its use will lead to greater uncertainty in the decay parameters. Consequently, we have tried to minimize the data collection time by optimizing instrumental conditions, while simultaneously collecting sufficient counts to resolve multiexponential decays. We have also tried to reduce systematic instrumental errors. The contemporaneous mode of data collection minimizes errors due to drift in the nanosecond flash lamp and the electronics. The use of standards monitors reproducibility of a monoexponential decay. Comparison of the fluorescence lifetime determined from the total fluorescence and from an experiment with the excitation polarizer in the magic-angle position provides a check for errors introduced by differences between the two sample cuvettes and by the normalization factor. In all experiments the error in fluorescence lifetimes is about ± 0.1 ns and in rotational correlation times about $\pm 5\%$. The temperature is regulated within $\pm 1°$.

IV. RESULTS

We have measured the decay of $I_V(t)$ and $I_H(t)$, as well as decay proportional to total fluorescence $I(t)$, for perylene and 9-aminoacridine in glycerol at different temperatures from 10 to 40 °C. Excitation wavelengths for perylene were $\lambda_{ex}=430$ and 256 nm, and the emission wavelength was $\lambda_{em}=448$ nm. Excitation wavelengths for 9-aminoacridine were $\lambda_{ex}=430$ and 260 nm, and the emission wavelength was $\lambda_{em}=460$ nm. In both compounds this corresponds to excitation into the lowest vibrational band of the first, positively polarized $\pi\rightarrow\pi^*$ transition and into the maximum of a higher, negatively polarized $\pi\rightarrow\pi^*$ transition. Additional excitation wavelengths for 9-aminoacridine were $\lambda_{ex}=317$ nm, corresponding to a weak, negatively polarized absorption region, and $\lambda_{ex}=404$, 381, and 358 nm, presumably higher vibrational bands of the first electronic transition (Fig. 4).

In all cases, the fluorescence decay is monoexponential and the fluorescence lifetime τ is essentially independent of temperature and excitation wavelength. The lifetimes of perylene varied from 4.5 to 4.8 ns and of 9-aminoacridine from 12.4 to 12.9 ns, slightly more than the experimental error. We have also measured the fluorescence decay of perylene and 9-aminoacridine at a single excitation wavelength $\lambda_{ex}=404$ nm and different emission wavelengths. The decay is monoexponential and the lifetime constant for emission wavelengths beyond the region of overlap of the absorption and emission spectra ($\lambda_{cm}>445$ nm for perylene; $\lambda_{cm}>437$ nm for 9-aminoacrodine). However, for emission wavelengths within the overlap region, we found significant deviations from monoexponential decay, with larger deviations at lower temperatures. We are unable to explain this observation.

The decay of the emission anisotropy was analyzed according to mono- or biexponential functions. Assuming monoexponential decay, we obtained a single rotational correlation time ϕ at each temperature and excitation wavelength. For both perylene and 9-aminoacridine, the value of ϕ depends not only on temperature but also on excitation wavelength (Tables I and II). The wavelength dependence exceeds the experimental error in each case, though it is more dramatic for perylene than for 9-aminoacridine. Furthermore, the large values of the reduced chi square χ_r^2 for the perylene data (particularly at $\lambda_{ex}=256$ nm) indicate that the assumption of monoexponential decay of the emission anisotropy is inadequate. We reasoned that the wavelength dependence of the single rotational correlation time ϕ is caused by anisotropic rotations, so that the apparent decay parameters obtained from the analysis according to a monoexponential are effective averages of the parameters of the true multiexponential decay. In the case of biexponential decay of the emission anisotropy, the apparent monoexponential decay parameters at early times (or equivalently for $\phi_1, \phi_2>\tau$) are given approximately by

$$\langle\beta\rangle\approx\beta_1+\beta_2\ , \tag{11a}$$

$$\langle\phi\rangle^{-1}\approx\frac{\beta_1/\phi_1+\beta_2/\phi_2}{\langle\beta\rangle}\ . \tag{11b}$$

Therefore, we attempted to analyze the data assuming biexponential functions for the decay of the emission anisotropy. It should be noted that accurate determination of the parameters of a multiexponential decay curve

Downloaded 01 May 2008 to 150.131.77.142. Redistribution subject to AIP license or copyright; see http://jcp.aip.org/jcp/copyright.jsp

TABLE I. Emission anisotropy decay parameters for perylene.

			Monoexponential analysis			Biexponential analysis				
T (°C)	λ_{ex} (nm)	$\langle r \rangle$	β	ϕ (ns)	χ_r^2	β_1	ϕ_1 (ns)	β_2	ϕ_2 (ns)	χ_r^2
10	256	−0.097	−0.16	7.4	1.6	0.10	114	−0.25	15.6	1.3
	430	0.285	0.34	22.7	1.2	0.10	114	0.25	15.2	1.1
15	256	−0.076	−0.16	4.3	2.8	0.10	70	−0.25	9.7	1.1
	430	0.260	0.34	14.9	1.2	0.10	70	0.25	9.7	1.0
20	256	−0.052	−0.16	2.5	5.8	0.10	45	−0.24	6.4	1.3
	430	0.231	0.33	10.5	1.5	0.10	45	0.24	6.4	1.1
25	256	−0.031	−0.17	1.5	10.8	0.10	28	−0.24	4.1	1.1
	430	0.197	0.33	7.1	2.0	0.10	28	0.24	4.1	1.1
30	256	−0.015	−0.19	0.8	11.7	0.10	17	−0.24	2.7	1.2
	430	0.165	0.32	5.1	2.6	0.10	17	0.24	2.7	1.1
35	256	~0	...	...	...	...	...	...	...	...
	430	0.137	0.29	4.1	2.5	0.10	13	0.24	1.7	1.2
40	256	~0	...	...	...	...	...	...	...	...
	430	0.111	0.27	3.2	2.8	0.10	9	0.24	1.1	1.1

is a difficult problem, due to the high degree of correlation among the parameters. This problem is accentuated in the case of the emission anisotropy because of the relatively fewer counts in the difference curve $D(t)$ and uncertainties in the parameters of the impulse response of the total fluorescence $s(t)$. However, by using auxillary information about one or more parameters, significant improvement in the accuracy of the remaining parameters may be expected. Here we illustrate how recovery of the decay parameters for the emission anisotropy is facilitated by considering data at two excitation wavelengths along with information about the transition dipole directions. The logic behind our approach and the results for perylene and 9-aminoacridine are described in the following sections.

A. Emission anisotropy of perylene

The transition dipoles of perylene lie in the plane of the aromatic rings; the absorption dipole at 430 nm is

TABLE II. Emission anisotropy decay parameters for 9-aminoacridine.

			Monoexponential analysis			Biexponential analysis				
T (°C)	λ_{ex} (nm)	$\langle r \rangle$	β	ϕ (ns)	χ_r^2	β_1	ϕ_1 (ns)	β_2	ϕ_2 (ns)	χ_r^2
10	260	−0.138	−0.16	80.6	1.3	−0.16	80.6			1.3
	317	−0.103	−0.12	92.2	1.1	−0.19	80.6	0.08	67.0	1.1
	430	0.292	0.35	69.7	1.1	0.07	80.6	0.27	67.0	1.1
15	260	−0.126	−0.16	52.2	1.2	−0.16	52.2			1.2
	317	−0.097	−0.12	59.1	1.1	−0.19	52.2	0.07	43.0	1.1
	430	0.269	0.34	44.8	1.1	0.07	52.2	0.27	43.0	1.1
20	260	−0.116	−0.16	35.0	1.0	−0.16	35.0			1.0
	317	−0.088	−0.12	39.8	1.1	−0.16	35.0	0.05	26.0	1.1
	358	0.177	0.26	27.8	1.2	0.06	35.0	0.20	26.0	1.2
	381	0.201	0.29	27.8	1.2	0.05	35.0	0.24	26.0	1.2
	404	0.222	0.32	27.6	1.1	0.07	35.0	0.26	26.0	1.1
	430	0.236	0.34	27.6	1.1	0.07	35.0	0.27	26.0	1.1
25	260	−0.098	−0.16	21.9	1.1	−0.16	21.9			1.1
	317	−0.077	−0.12	24.6	1.1	−0.16	21.9	0.05	16.0	1.0
	430	0.198	0.35	17.1	1.0	0.07	21.9	0.27	16.0	1.0
30	260	−0.083	−0.16	14.1	1.2	−0.16	14.1			1.2
	317	−0.067	−0.12	16.3	1.1	−0.18	14.1	0.06	10.0	1.0
	430	0.161	0.34	11.2	1.1	0.07	14.1	0.27	10.0	1.0
35	260	−0.066	−0.16	9.0	1.1	−0.16	9.0			1.1
	317	−0.052	−0.12	9.3	1.1	−0.14	9.0	0.02	7.0	1.1
	430	0.125	0.34	7.5	1.1	0.07	9.0	0.27	7.0	1.1
40	260	−0.053	−0.16	6.0	1.1	−0.16	6.0			1.1
	317	−0.040	−0.12	6.2	1.0	−0.14	6.0	0.02	4.8	1.1
	430	0.096	0.34	5.1	1.2	0.07	6.0	0.27	4.8	1.2

Downloaded 01 May 2008 to 150.131.77.142. Redistribution subject to AIP license or copyright; see http://jcp.aip.org/jcp/copyright.jsp

TABLE III. Recovery of emission anisotropy decay parameters from synthetic data.

	Synthetic parameters				Recovered parameters			
	β_1	ϕ_1 (ns)	β_2	ϕ_2 (ns)	β_1	ϕ_1 (ns)	β_2	ϕ_2 (ns)
Perylene	0.1	70	−0.25	9.7	0.09	88.7	−0.24	9.6
	0.1	70	0.25	9.7	0.08	111	0.26	9.8
	0.1	28	−0.24	4.1	0.1	26.5	−0.25	4.2
	0.1	28	0.24	4.1	0.09	31.7	0.25	4.2
	0.1	13	0.24	1.7	0.1	14.2	0.24	1.8
9-Aminoacridine	0.07	80.6	0.27	67.0	0.09	98	0.26	63.5
	0.07	35.0	0.27	26.0	0.03	41	0.30	26.5
	0.07	9.0	0.27	7.0	0.07	7.4	0.27	7.4

directed along the long axis of the molecule, and at 256 nm along the short axis (Fig. 1).[27] Thus, at $\lambda_{ex}=430$ nm the absorption and emission dipoles are parallel, whereas at $\lambda_{ex}=256$ nm they are perpendicular. Assuming that the molecule can be modeled as an ellipsoid of revolution, the location of the diffusion principal axes may be deduced from the relative values of the single rotational correlation time ϕ at the two excitation wavelengths. The wavelength dependence of $\langle\phi\rangle$ is predicted for various cases from Eq. (11b), with values of β_1 and β_2 estimated from Eq. (3) and relative values of ϕ_1 and ϕ_2 from Eq. (4). If perylene rotated as a prolate with symmetry axis parallel to the long axis of the molecule ($\theta_e=0$), then the decay of the emission anisotropy would be monoexponential with the same rotational correlation time (ϕ_1) at both excitation wavelengths and $\langle\phi\rangle_{430}=\langle\phi\rangle_{256}$. On the other hand, if perylene rotated as an oblate with symmetry axis perpendicular to the plane of the rings ($\theta_a=\theta_e=90°$), then $\langle\phi\rangle_{430}\approx\langle\phi\rangle_{256}$ for the sticking boundary condition ($\phi_1\approx\phi_2$), but $\langle\phi\rangle_{430}>\langle\phi\rangle_{256}$ for the slipping boundary condition ($\phi_1\gg\phi_2$). Since the values of ϕ in Table I at $\lambda_{ex}=430$ nm are greater than those at $\lambda_{ex}=256$ nm, we concluded that perylene rotates as a disk with the slipping boundary condition. In this case the emission anisotropy at the two excitation wavelengths should take the following forms:

$$r(t)=\beta_1\exp(-t/\phi_1)+\beta_2\exp(-t/\phi_2)\,,\quad \lambda_{ex}=430\text{ nm}\,, \tag{12a}$$

$$r(t)=\beta_1\exp(-t/\phi_1)-\beta_2\exp(-t/\phi_2)\,,\quad \lambda_{ex}=256\text{ nm}\,, \tag{12b}$$

with the same values of β's and ϕ's in both equations and with $\phi_1>\phi_2$. Therefore, we searched for a set of four parameters β_1, ϕ_1, β_2, and ϕ_2 which satisfies the experimental data at both excitation wavelengths. We also required that individual fits to the data for a biexponential were better (lower values of χ_r^2 and improved shape of the autocorrelation function) than the best fit for a monoexponential. The final parameters for the decay of the emission anisotropy of perylene are presented in Table I. The analysis according to biexponential functions yields pre-exponentials that are essentially independent of temperature but dependent on excitation wavelength and rotational correlation times that are dependent on temperature but independent of excitation wavelength. This contrasts with analysis according to a monoexponential, where both parameters are temperature and wavelength dependent.

The advantage as well as the validity of our method was assessed with synthetic data. Computer-simulated data with Poisson noise were generated, using parameters for biexponential decay of the emission anisotropy from Table I and the corresponding decay of total fluorescence. These data were analyzed in terms of a biexponential for the emission anisotropy with no restrictions. The examples in Table III show that the parameters are not recovered accurately even in the ideal case. The synthetic data were also analyzed in terms of a monoexponential for the emission anisotropy. The values of β, ϕ, and χ_r^2 agreed with those obtained from monoexponential analysis of the experimental data.

The anisotropic character of the rotation of perylene is so pronounced that the decay of the emission anisotropy can take unusual forms. The experimental data for the emission anisotropy at $\lambda_{ex}=256$ nm and 30 °C are depicted in Fig. 2. Figure 2(A) shows the experimental emission anisotropy curve $R(t)=D(t)/S(t)$ together with the best fit for a monoexponential; this fit is clearly unacceptable. Figure 2(B) shows the fit for a biexponential; the value of χ_r^2 as well as the autocorrelation function (not shown) indicate an excellent fit to the data. The negative emission anisotropy at early times is due to the orthogonality of the absorption and emission dipoles. The fact that the emission anisotropy becomes positive with time prior to decaying to zero demonstrates that rotation within the plane of the aromatic rings is faster than rotation out of plane (i.e., $D_{\parallel}>D_{\perp}$). The oscillatory behavior of the emission anisotropy is described by Eq. (12b). Although such decay functions have been predicted theoretically, to the best of our knowledge this is the first reported observation of oscillating decay of the emission anisotropy. The physical basis of this phenomenon is readily apparent from the impulse response functions for the perylene data, which are shown in Fig. 3. In order for the emission anisotropy to change sign, the relative magnitudes of the vertically and horizontally polarized components of the emission intensity must invert with time [Fig. 3(A)]. For perylene at $\lambda_{ex}=256$ nm, those molecules whose aromatic rings are aligned with absorption dipole (short axis) parallel, and consequently emission

Downloaded 01 May 2008 to 150.131.77.142. Redistribution subject to AIP license or copyright; see http://jcp.aip.org/jcp/copyright.jsp

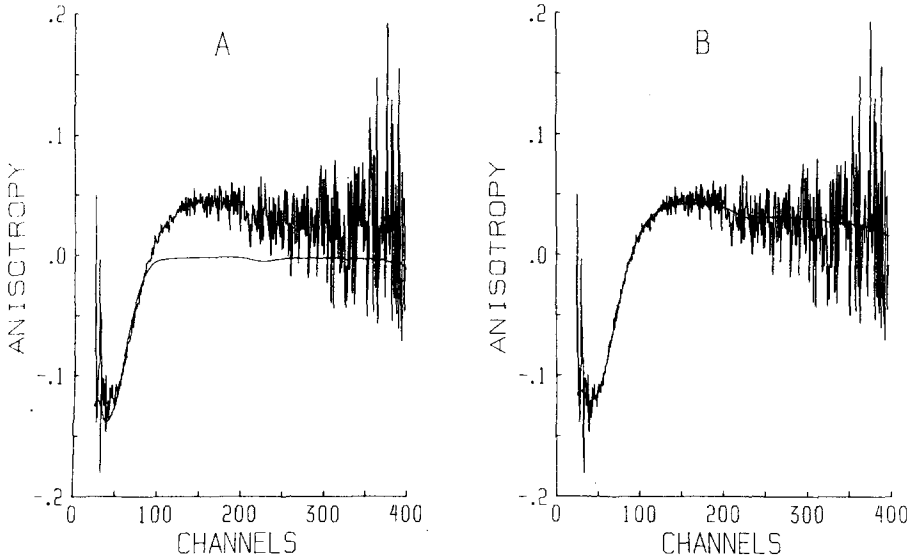

FIG. 2. Experimental and computed decay of emission anisotropy of perylene. $\lambda_{ex} = 256$ nm, $\lambda_{em} = 448$ nm, 30°C. The experimental emission anisotropy curve $R(t) = D(t)/S(t)$ is compared with the quotient of the convolved impulse response for the difference $d(t) = s(t) \cdot r(t)$ and the sum $s(t) = 2.6 \exp(-t/4.55\ \text{ns})$. (A) Monoexponential $r(t) = 0.19 \exp(t/0.8\ \text{ns})$, $\chi_r^2 = 11.7$. (B) Biexponential $r(t) = 0.10 \exp(-t/17\ \text{ns}) - 0.24 \exp(t/2.7\ \text{ns})$, $\chi_r^2 = 1.2$.

dipole (long axis) perpendicular, to the electric vector of the exciting light are photoselected. The initial horizontal intensity is greater than the vertical intensity so that the emission anisotropy is negative. At very early times the fast rotation in the plane of the rings moves the emission dipoles in the vertical direction, causing the horizontal intensity $i_H(t)$ to decrease rapidly and the vertical intensity $i_V(t)$ to increase slightly (even though the total emission intensity decays). If the in-plane rotation were sufficiently fast compared to the out-of-plane rotation, the emission anisotropy could rise to a value of 0.1 (the average of the values for emission dipoles oriented in the vertical and horizontal directions). In the case of perylene, the maximum emission anisotropy is somewhat lower, due to the slow rotation out of plane which depolarizes the fluorescence emission at later times [Fig. 3(B)].

B. Emission anisotropy of 9-aminoacridine

For the two strong absorption bands of 9-aminoacridine centered at about 405 and 260 nm, the transition dipoles lie in the plane of the rings. At 430 nm the absorption dipole is directed along the short axis of the molecule, and at 260 nm along the long axis (Fig. 1).[28] The first electronic transition shows descending emission anisotropy across the absorption band at lower wavelengths (Fig. 4) and across the emission band at higher wavelengths (data not shown). A similar wavelength dependence was observed in frozen ethanol/ether solution.[29] Such behavior is explained in the case of anthracene by the finding that the absorption dipole direction of the first $\pi \rightarrow \pi^*$ transition exhibits an increasing amount of long-axis component at higher vibronic levels.[30] By analogy, then, the emission dipole of 9-aminoacridine at 460 nm would not be collinear with the absorption dipole at 430 nm. The angle δ between absorption and emission dipoles can be estimated from the limiting emission anisotropy $r_0 = 0.2\ (3\cos^2\delta - 1)$. Based on the steady-state emission anisotropies in frozen solution ($r_0 = 0.35$ at 430 nm and $r_0 = -0.15$ at 260 nm) and the above absorption dipole directions, we estimate that the emission dipole is directed about 17° from the short axis of the molecule and 73° from the long axis. This is in

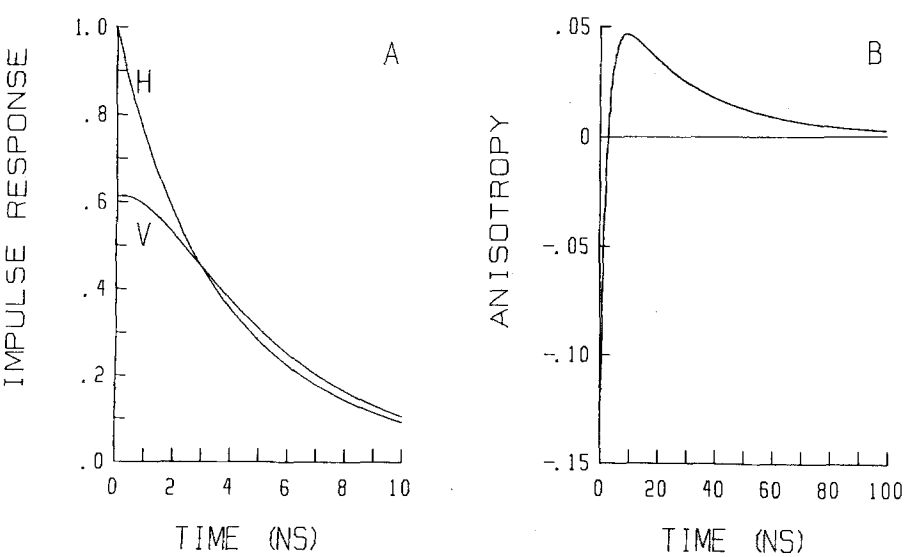

FIG. 3. Impulse response (deconvolved decay) of perylene for biexponential decay of the emission anisotropy from the experiment in Fig. 2. (A) Decay of $i_{VV}(t)$ and $i_{HV}(t)$. (B) Decay of $r(t)$.

Downloaded 01 May 2008 to 150.131.77.142. Redistribution subject to AIP license or copyright; see http://jcp.aip.org/jcp/copyright.jsp

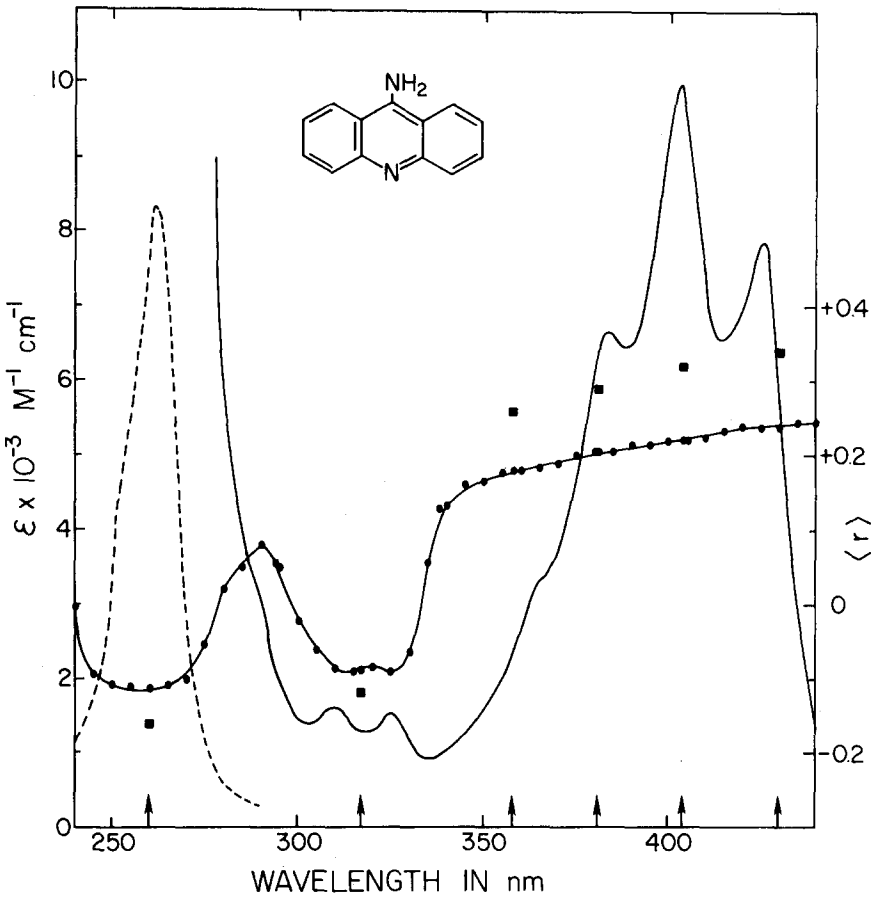

FIG. 4. Absorption and emission anisotropy spectra of 9-aminoacridine in glycerol at 20°C. (—) molar extinction coefficient ϵ; (- - - -) 0.1 ϵ; (● — ●) steady state emission anisotropy, $\lambda_{em}=460$ nm; (■) r_0 value from Table II, λ_{ex} indicated by arrow.

agreement with the corresponding angles of 18° and 77°, respectively, calculated from the initial emission anisotropies in our time-resolved measurements ($r_0=0.34$ at 430 nm and $r_0=-0.16$ at 260 nm; Table II).

In the case of 9-aminoacridine, the relatively small wavelength dependence of the single rotational correlation time ϕ as well as the absence of apparent deviations from monoexponential decay ($\chi_r^2=1.0$–1.3) indicate that the rotation is only slightly anisotropic. As before, the location of the diffusion principal axes is inferred from the relative values of ϕ at $\lambda_{ex}=430$ and 260 nm. We can discard models in which 9-aminoacridine rotates as an oblate with symmetry axis perpendicular to the plane of the aromatic rings because the values of ϕ in Table II at $\lambda_{ex}=430$ nm are less than those at $\lambda_{ex}=260$ nm. For oblates with the sticking or slipping boundary condition, $\langle\phi\rangle_{430}$ should be greater than $\langle\phi\rangle_{260}$ as in the case of perylene. However, if 9-aminoacridine rotated as a prolate with symmetry axis parallel to the long axis of the molecule, then $\langle\phi\rangle_{430}<\langle\phi\rangle_{260}$ as observed. The decay of the emission anisotropy should be biexponential at $\lambda_{ex}=430$ nm ($\theta_a=90°$) and monoexponential at $\lambda_{ex}=260$ nm ($\theta_a=0°$). The appropriate equations are

$$r(t)=\beta_1\exp(-t/\phi_1)+\beta_2\exp(-t/\phi_2)\,, \quad \lambda_{ex}=430\text{ nm}\,, \tag{13a}$$

$$r(t)=\beta_1\exp(-t/\phi_1)\,, \quad \lambda_{ex}=260\text{ nm}\,, \tag{13b}$$

with the same values of ϕ_1 in both equations and with $\phi_1>\phi_2$. The numerical value of β_1 in the two equations is different and $\beta_1<\beta_2$ in Eq. (13a). Although the magnitudes of ϕ_1 and ϕ_2 are expected to be much closer than in the case of perylene, ϕ_1 can be obtained quite accurately from the monoexponential decay at $\lambda_{ex}=260$ nm. Our strategy for recovering the decay parameters of 9-aminoacrodine was thus to (1) determine ϕ_1 from the data at $\lambda_{ex}=260$ nm; (2) using this value of ϕ_1 along with estimated β's in Eq. (13a), determine ϕ_2 from the data at $\lambda_{ex}=430$ nm; and (3) then, using these values of the ϕ's, determine the β's at other excitation wavelengths. We required that the values of χ_r^2 obtained from biexponential analysis were less than or equal to those from the monoexponential analysis. The best values of β_1 and β_2 at $\lambda_{ex}=430$ nm are presented in Table II; they are very close to those predicted for the geometry described above.

The rotational correlation times for 9-aminoacridine only differ by about 30%, so it is not surprising that the anisotropic rotation is masked in measurements at a single excitation wavelength. Figure 5 shows the experimental data for the emission anisotropy at $\lambda_{ex}=430$ nm and 25 °C. The experimental difference curve $D(t)$ together with the best fit to a monoexponential and the fit to a biexponential are depicted in panels (A) and (B), respectively. Obviously, both fits are excellent, and the statistical criteria offer no help in deciding between the two. In general, one might expect the determination of multiexponential decays whose time constants differ by less than a factor of 2 to be tenuous at best.[31] The necessity of utilizing independent information to obtain the parameters for the biexponential decay of the emis-

Downloaded 01 May 2008 to 150.131.77.142. Redistribution subject to AIP license or copyright; see http://jcp.aip.org/jcp/copyright.jsp

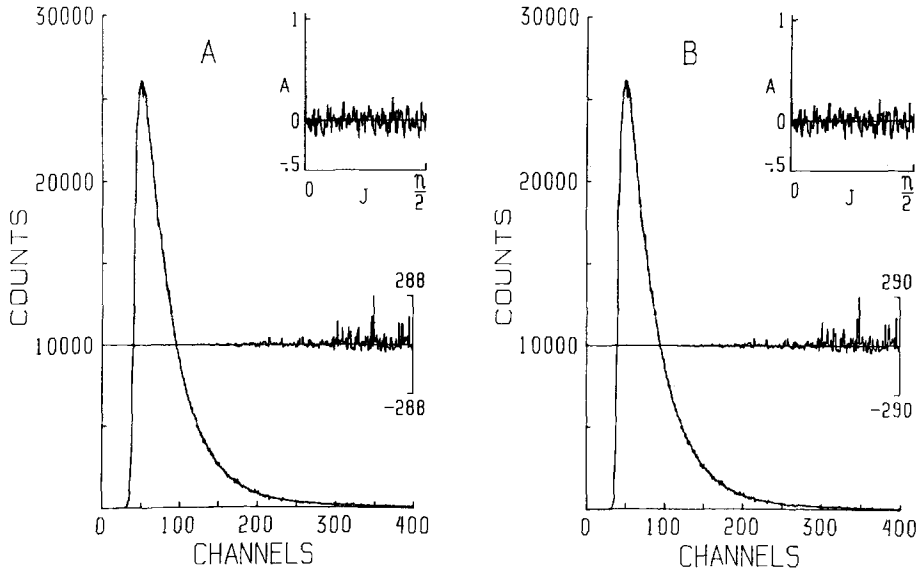

FIG. 5. Difference curve of 9-aminoacridine. Timing calibration 0.206 ns/channel, $\lambda_{ex}=430$ nm, $\lambda_{em}=460$ nm, 25°C. The weighted percent residuals and the autocorrelation function of the residuals (inset) are also shown. (A) Monoexponential fit $\beta=0.35$, $\phi=17.1$ ns, $\chi_r^2=1.0$. (B) Biexponential fit $\beta_1=0.07$, $\phi_1=21.9$ ns, $\beta_2=0.27$, $\phi_2=16.0$ ns, $\chi_r^2=1.0$.

sion anisotropy of 9-aminoacridine can be demonstrated with synthetic data. As in the case of perylene, computer-simulated data were generated taking parameters from Table II. The results of a biexponential analysis with unrestricted parameters are given in Table III. It is evident from the poor recovery in the ideal case that such analysis would be impossible in the real case. In addition, monoexponential analysis of the synthetic data yielded the same values of β and ϕ as the exponential data.

Having determined ϕ_1 and ϕ_2 for 9-aminoacridine from the experiments at excitation wavelengths where we are reasonably certain of exciting single transitions of known direction, we can use the rotational correlation times to aid in the recovery of decay parameters at excitation wavelengths for which we have no additional information. For the experiments at $\lambda_{ex}=317$ nm, the single rotational correlation time ϕ obtained from the monoexponential analysis was larger than either ϕ at $\lambda_{ex}=430$ or 260 nm. We deduced from Eq. (11) that this would happen only if ϕ_1 had a larger, negative pre-exponential and ϕ_2 a smaller, positive pre-exponential in a multiexponential decay. In order to rationalize the data at $\lambda_{ex}=317$ nm, we assumed that the absorption dipole does not lie along a principal diffusion axis so that the emission anisotropy is a sum of three exponentials. However, because the values of $D_\perp$ and $D_\parallel$ for 9-aminoacridine are so close (Table IV), the longer rotational correlation times $\phi_1=(6D_\perp)^{-1}$ and $\phi_3=(5D_\perp+D_\parallel)^{-1}$ are indistinguishable and slightly different from the shorter rotational correlation time $\phi_2=(2D_\perp+4D_\parallel)^{-1}$. The decay of the emission anisotropy at $\lambda_{ex}=317$ nm would still be biexponential as in Eq. (13a) but with the following pre-exponentials:

$$\beta_1=0.1(3\cos^2\theta_a-1)(3\cos^2 73^\circ-1)+1.2\sin\theta_a\cos\theta_a\sin 73^\circ\cos 73^\circ\cos\psi_{ae}\,, \quad (14a)$$

$$\beta_2=0.3\sin^2\theta_a\sin^2 73^\circ\cos 2\psi_{ae} \quad (14b)$$

where the emission dipole angle $\theta_e=73^\circ$ has been explicitly introduced. The best values of the β's determined from the biexponential analysis are given in Table II. Although the limiting emission anisotropy $r_0=\beta_1+\beta_2$ is independent of temperature, the values of β_1 and β_2 fluctuate somewhat. The best estimate of the absorption dipole direction at 317 nm obtained from Eq. (14) and the experimental β's is $\theta_a\approx 5$–6° and $\psi_{ae}\approx 20^\circ$. For the experiments at $\lambda_{ex}=404$, 381, and 358 nm, we assumed that the absorption dipoles lie in the plane of the rings ($\psi_{ae}=0$) as expected for higher vibrational bands of the first $\pi\rightarrow\pi^*$ transition. Here again the decay of the emission anisotropy would be practically biexponen-

TABLE IV. Principal diffusion coefficients of perylene and 9-aminoacridine in glycerol.

	Perylene		9-Aminoacridine	
T (°C)	$D_\parallel\times10^{-7}$ (s^{-1})	$D_\perp\times10^{-6}$ (s^{-1})	$D_\parallel\times10^{-6}$ (s^{-1})	$D_\perp\times10^{-6}$ (s^{-1})
10	1.5	1.5	2.7	2.1
15	2.5	2.4	4.2	3.2
20	3.7	3.7	7.2	4.8
25	5.8	6.0	12	7.6
30	8.8	9.8	19	12
35	14	13	27	19
40	22	19	38	28
Ratio $D_\parallel/D_\perp$	10 ± 1		1.4 ± 0.1	

Downloaded 01 May 2008 to 150.131.77.142. Redistribution subject to AIP license or copyright; see http://jcp.aip.org/jcp/copyright.jsp

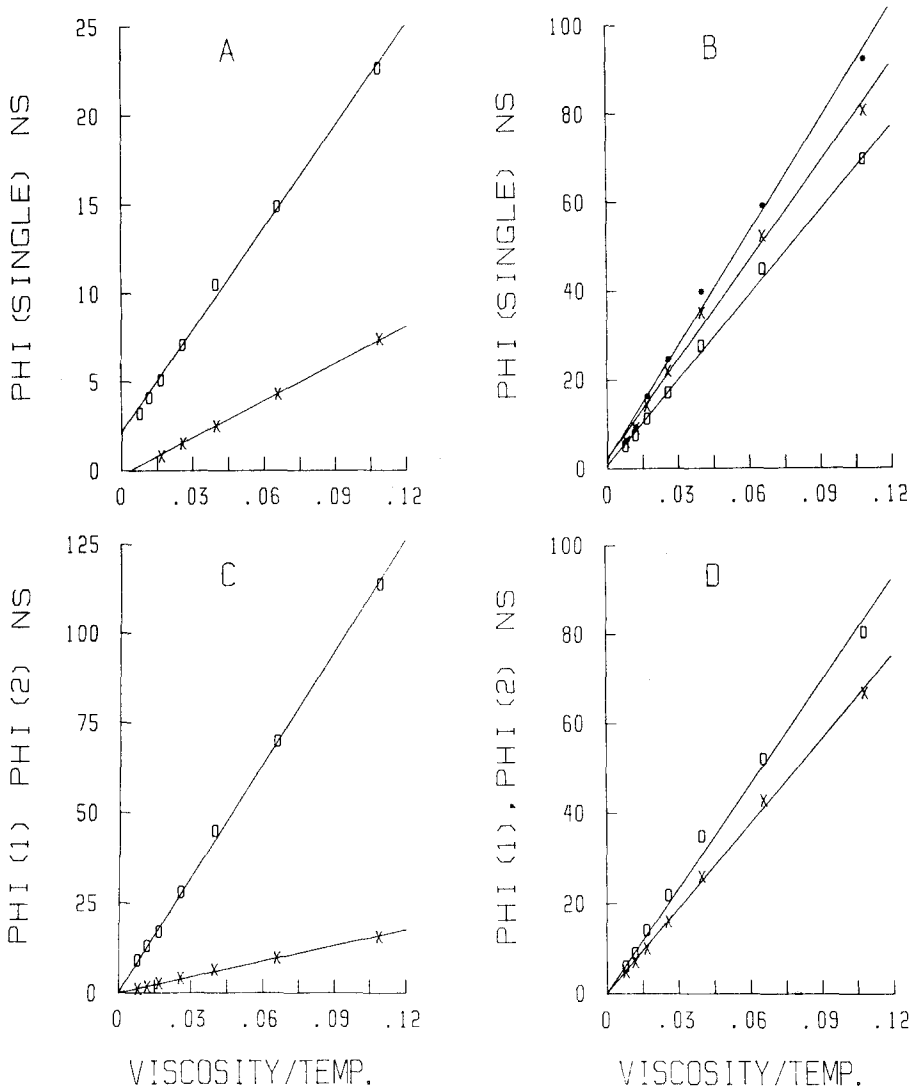

FIG. 6. Dependence of rotational correlation times on viscosity and temperature. Viscosities of 99% glycerol (w/w) in P taken from the literature.[33] Plots of ϕ vs η/T. Lines drawn are least squares fit to the data. (A) Perylene: (□) $\lambda_{ex}=430$ nm; (×) $\lambda_{ex}=256$ nm. (B) 9-Aminoacridine: (□) $\lambda_{ex}=430$ nm; (*) $\lambda_{ex}=317$ nm; (×) $\lambda_{ex}=260$ nm. Plots of ϕ_1 and ϕ_2 vs η/T. Lines drawn are least squares fit of the data to the straight line $\phi=\text{const}\cdot\eta/T$. (□) ϕ_1; (×) ϕ_2. (C) Perylene. (D) 9-Aminoacridine.

tial with the following pre-exponentials:

$$\beta_1 = 0.1(3\cos^2\theta_a - 1)(3\cos^2\theta_e - 1) + 1.2\sin\theta_a\cos\theta_a\sin\theta_e\cos\theta_e\,, \tag{15a}$$

$$\beta_2 = 0.3\sin^2\theta_a\sin^2\theta_e\,. \tag{15b}$$

The best values of β_1 and β_2 obtained from the data at these excitation wavelengths are in good accord with those calculated from Eq. (15) using transition dipole directions estimated from the steady-state emission anisotropies in frozen solution[29] and considering spatial oscillators.[32]

C. Rotational dynamics of perylene and 9-aminoacridine

The dependence of the rotational correlation times of perylene and 9-aminoacridine on viscosity and temperature is protrayed in Fig. 6. Panels (A) and (B) show the apparent single rotational correlation time ϕ at different excitation wavelengths plotted vs η/T. Evidently, ϕ is a linear function of η/T in all cases, though the least squares lines do not intersect the origin. Panels (C) and (D) show the plots of the true rotational correlation times ϕ_1 and ϕ_2. Here, too, a linear dependence on η/T is obtained, but with good fit to a line passing through the origin. The highly anisotropic rotation of perylene is manifest in the large difference in slopes for ϕ_1 and ϕ_2 [panel (C)]. Moreover, $\phi_{\perp}$, which is dominated by the in-plane rotation rate $D_{\parallel}$ [Eq. (4)], is relatively insensitive to η/T. In contrast, ϕ_1, which is governed by the out-of-plane rotation rate $D_{\perp}$, is strongly dependent on solution conditions. This behavior implies that the molecule rotates somewhat independently of its solvent layer. On the other hand, the slopes for 9-aminoacridine are not very different [panel (D)]. Both ϕ_1 and ϕ_2 depend strongly on η/T, indicating substantial coupling of the rotations to the solvent. The compounds investigated here pose experimental problems of opposite nature which are circumvented by excitation of differently oriented absorption oscillators. In the case of perylene, the rotation is sufficiently anisotropic that it is readily detected at a single excitation wavelength. However, because the rotational correlation times are so different, both ϕ_1 and ϕ_2 will be reliably determined only under limited conditions. As indicated from synthetic data (Table III), the rotational correlation time associated with the larger pre-expo-

Downloaded 01 May 2008 to 150.131.77.142. Redistribution subject to AIP license or copyright; see http://jcp.aip.org/jcp/copyright.jsp

nential would be recovered more accurately. Since the fluorescence lifetime is about 5 ns, it would normally be possible to measure rotational correlation times up to about 50 ns. Yet, judging from the fact that the values of ϕ_1 at high viscosity fall on the straight line in Fig. 6(C), we have apparently obtained good values over twice that range. In the case of 9-aminoacridine, the situation is reversed. Both rotational correlation times are accessible within the about 13 ns fluorescence lifetime. However, because the values of ϕ_1 and ϕ_2 are very similar, the anisotropic rotation is not detected in experiments at only one excitation wavelength.

The principal diffusion coefficients of perylene and 9-aminoacridine in glycerol were calculated from the rotational correlation times ϕ_1 and ϕ_2 according to Eq. (4) and put into Table IV. The ratio of the diffusion coefficients for the in-plane and out-of-plane rotations of perylene $D_{\parallel}/D_{\perp}$ is 10 ± 1. This is in excellent agreement with the value of 10 ± 2 obtained by Zinsli from the time-resolved emission anisotropy in paraffin over the temperature range -20 to $50\,^{\circ}C$.[4] It is also in qualitative accord with estimates based on steady-state,[12] phase,[7] and lifetime-resolved[13] fluorescence depolarization measurements under a variety of solution conditions. For 9-aminoacridine, the ratio of the diffusion coefficients about the major and minor axes $D_{\parallel}/D_{\perp}$ is 1.4 ± 0.1. This slightly anisotropic rotation was not observed in a previous study by differential phase fluorimetry.[7]

The magnitudes of the r_0 values obtained from the time-resolved emission anisotropies are somewhat lower than the theoretical values for parallel ($r_0 = 0.4$) or perpendicular ($r_0 = -0.2$) absorption and emission oscillators. However, recent measurements using picosecond laser excitation have yielded the maximum value of $r_0 = 0.4$ for a few dyes.[34,35] The initial emission anisotropies of perylene ($r_0 = 0.35$ at 430 and $r_0 = -0.15$ at 256 nm) agree with the limiting values determined in propylene glycol at about $-50\,^{\circ}C$.[12,13] Furthermore, the magnitude of the pre-exponential β_2 but not β_1 is less than the expected value (Table I). These two observations are consistent with an emission dipole direction of about 17° from the long axis of the molecule. Alternatively, since β_2 is associated with the fast in-plane rotation, the depolarization might result from an ultrafast in-plane libration, which is beyond the resolution of our instrument. While we cannot rule out a similar explanation in the case of 9-aminoacridine, the evidence discussed in this and the preceding section indicates that the depolarization probably reflects the emission dipole orientation.

V. DISCUSSION

Fluorescence depolarization is an important method for studying the rotational dynamics of small and large molecules. Several criteria have been used to infer that in some cases the rotation is anisotropic. This may have its origin in the shape of the molecule or in the anisotropic nature of its environment. Evidence for deviations from isotropic behavior usually depends on varying one or more conditions such as solvent viscosity, temperature, or fluorescence lifetime. Anisotropic rotations give rise to curvature in the Perrin plots of steady-state fluorescence data.[11] If the rotation rates are sufficiently different, they can be selectively observed by adding a quencher. This lifetime-resolved emission anisotropy is a steady-state analog of the time-resolved emission anisotropy. Lakowicz and Knutson[13] investigated perylene rotations in propylene glycol at 26 °C by lifetime-resolved measurements and estimated $D_{\parallel}/D_{\perp}$ in the range of 1 to 10. Theoretical work by Jabtoński suggested that phase techniques could also be used to study rotational motion.[37] Weber has developed phase fluorimetry into a powerful method for detecting anisotropic rotations.[14] He showed that the maximum differential tangent obtained for anisotropic rotators is lower than the value expected for a sphere. By fitting various models to the phase data, Mantulin and Weber estimated $D_{\parallel}/D_{\perp} \approx 28$ for perylene in propylene glycol.[7] However, they concluded that 9-aminoacridine and other aromatics capable of forming hydrogen bonds with the solvent rotate isotropically. Although these fluorescence techniques are quite sensitive to anisotropic rotations, small deviations from isotropic behavior may not be detectable within the experimental error. The information content of steady-state as well as pulse measurements can be augmented by excitation at wavelengths corresponding to different orientations of absorption and emission dipoles (different r_0 values). This changes the initial distribution of emission dipoles and thus alters the relative contribution of the different rotations to the depolarization. For anisotropic rotators the slope of the Perrin plot is dependent on excitation wavelength.[11] Shinitzky *et al.* showed that the anisotropic rotation of perylene can be demonstrated by varying the excitation wavelength in steady-state measurements at constant viscosity and temperature.[12] They estimated $D_{\parallel}/D_{\perp} > 10$ for perylene in propylene glycol at $-14\,^{\circ}C$ and in propylene glycol/glycerol at 4 °C.

Pulse fluorimetry has not been extensively used to study rotational diffusion of small molecules. Several investigators have reported deviations from Stokes–Einstein behavior of fluorescein derivatives in various solvents, which they attributed to different types of solvent–fluorophore interactions.[34,36] In the previous study of perylene, however, anisotropic rotation was identified from the biexponential decay of the emission anisotropy.[4] Biological systems afford more complex examples of rotational motions, such as segmental flexibility[38,39] and hindered rotations.[40,41] In addition, microheterogeneity in rotational behavior may be anticipated. Pulse measurements are of particular promise for distinguishing different models for rotational motion of a fluorophore. In theory, the parameters describing the decay of the emission anisotropy could be obtained from a single decay curve $I_V(t) = I(t)[1 + 2r(t)]$ or $I_H(t) = I(t)[1 - r(t)]$. In practice, the polarized fluorescence decay curves are distorted by instrumental artifacts such as convolution with the excitation profile, energy dependent distortions introduced by the detector, and photon pileup. Even in the absence of systematic er-

Downloaded 01 May 2008 to 150.131.77.142. Redistribution subject to AIP license or copyright; see http://jcp.aip.org/jcp/copyright.jsp

rors the information content would probably not be sufficient to discriminate between various mechanisms for rotational diffusion. The situation is improved if two decay curves $I_V(t)$ and $I_H(t)$ are collected and analyzed in terms of the sum curve $I_V(t)+2I_H(t)$ and the difference curve $I_V(t)-I_H(t)$. However, this procedure may still not provide definitive information about a rotating system. The present paper demonstrates that the amount of information can be significantly enhanced by combining data obtained at more than one excitation wavelength. Furthermore, if the oscillator directions are known, the pre-exponentials should change in a predictable way, thus reducing the number of degrees of freedom in the data analysis.

Our results show that the in-plane rotation rate of perylene $D_{\parallel}$ (Table IV) is about six times faster than expected from the Perrin theory [Eqs. (5b) and (6b)] for an oblate ellipsoid of the same size. This supports Mantulin and Weber's conclusion that the rotational behavior of unsubstituted aromatic hydrocarbons approximates a slipping rather than sticking boundary condition.[7] Hu and Zwanzig have treated rotational diffusion of ellipsoids with the slipping boundary condition, assuming free diffusion about the symmetry axis ($D_{\parallel}\to\infty$).[5] If we model perylene as a disk of thickness 3.5 Å based on the distance between molecular planes in the crystal[42] and use Hu and Zwanzig's theory to estimate the axial ratio from the out-of-plane rotation rates $D_{\perp}$ (Table IV), we obtain $\rho=0.3$ (thickness/diameter). This corresponds to a diameter of about 10 Å, which is 40%–50% larger than the carbon skeleton. Considering the crudeness of the approximations as well as the experimental error, the discrepancy is not unreasonable. Moreover, the in-plane rotation rate $D_{\parallel}$ is much slower than the free rotor value ($\approx 10^{11}$ s^{-1}). This may be due to the fact that the perylene molecule is not really a disk, and even the in-plane rotation must displace some solvent. Zinsli also studied perylene rotations by nanosecond pulse methods, exciting at 396 nm.[4] He interpreted his results according to a diffusional model involving rotational jumps and librational oscillations. In particular, Zinsli obtained temperature dependent pre-exponentials. However, we were able to fit the data at both excitation wavelengths to a more simple model with pre-exponentials independent of temperature (Table I).

The anisotropic rotation of 9-aminoacridine is entirely consistent with classical hydrodynamic theory [Eqs. (5) and (6a)]. Mantulin and Weber likewise concluded that this molecule rotates with the sticking boundary condition.[7] From the data in Table IV, we calculate the length of the major and minor axes of the prolate ellipsoid to be 7.2 and 4.8 Å, respectively (axial ratio $\rho=1.5$). These dimensions are very close to the actual molecular dimensions. The decay of the emission anisotropy appeared to be monoexponential at all excitation wavelengths, but the apparent single rotational correlation time was wavelength dependent. We considered several explanations for this effect in addition to anisotropic rotation. Chemical and spectral studies showed no evidence for impurities or aggregates. The excitation spectrum was independent of emission wavelength over the concentration range 10^{-5} to 10^{-6} M, and conversely the emission spectrum was independent of excitation wavelength. Heiss *et al.* reported a single rotational correlation time for perylene and rhodamine 6 G, which decreased at lower excitation wavelengths.[43] They interpreted this in terms of a local heating of the solvent by excess vibrational energy.[44] In the case of 9-aminoacridine, the wavelength dependence of ϕ is in the opposite direction. Further, our finding that the rotational correlation times ϕ_1 and ϕ_2 obtained from the biexponential analyses for perylene and 9-aminoacridine are independent of excitation wavelength rules out "local temperature" effects on the nanosecond time scale even for the very large energy excess between 260 and 430 nm. This agrees with other recent polarization data.[45] The possibility of supersolvation of 9-aminoacridine in a higher electronic state was also considered and ruled out.

VI. CONCLUSION

We have demonstrated in this paper that pulse fluorimetry is a suitable method for investigating the detailed mechanisms of rotational diffusion. It has been shown that excitation of differently oriented oscillators is one way to increase the information available from emission anisotropy data. The fluorescence measurements concern the rotational behavior of excited molecules. In the absence of an excited state conformational change this reflects the rotation of the parent ground state as well. The concepts developed here can also be applied to picosecond emission or absorption experiments.

Understanding of the rotational motion of molecules is important because it contributes to our knowledge of solvent structure and chemical reactivity. Continuum theories of hydrodynamics have normally been used to interpret rotational motion. As better experimental values of rotational diffusion coefficients become available, molecular mechanisms based on jump and collisional theories can be subjected to rigorous scrutiny. In biochemical systems the rotational behavior of fluorophores on proteins or substrates at active sites of enzymes is related to biological function. It is thus of value to have sufficient information content in experimental data to permit comparison with theoretical proposals.

ACKNOWLEDGMENTS

We are indebted to Dr. M. G. Badea and Mr. D. Walbridge who made the initial observations of the wavelength dependence of the single rotational correlation time ϕ of 9-aminoacridine. Their preliminary studies provided the impetus for the present work. We thank Dr. A. T. Swim for chemical and spectral measurements on 9-aminoacridine, Professor R. A. Laine for mass spectrometry, D. Walbridge for assistance with computations, and Ms. L. Hall for preparation of the manuscript. We also thank Professor I. Z. Steinberg and Dr. J. R. Knutson for helpful discussions. This work was supported by NIH research grants GM 22873 (M.D.B.) and GM 11632 (L.B). This is publication No. 1105 from the McCollum-Pratt Institute.

Downloaded 01 May 2008 to 150.131.77.142. Redistribution subject to AIP license or copyright; see http://jcp.aip.org/jcp/copyright.jsp

[1]W. J. Huntress, Jr., Adv. Magn. Reson. **4**, 1 (1970).
[2]S. A. Goldman, G. V. Bruno, C. F. Polnaszek, and J. H. Freed, J. Chem. Phys. **56**, 716 (1972).
[3]R. L. Vold, R. R. Vold, and D. Canet, J. Chem. Phys. **66**, 1202 (1977).
[4]P. E. Zinsli, Chem. Phys. **20**, 299 (1977).
[5]C.-M. Hu and R. Zwanzig, J. Chem. Phys. **60**, 4354 (1974).
[6]D. R. Bauer, G. R. Alms, J. I. Brauman, and R. Pecora, J. Chem. Phys. **61**, 2255 (1974).
[7]W. W. Mantulin and G. Weber, J. Chem. Phys. **66**, 4092 (1977).
[8]A. C. Albrecht, J. Mol. Spectrosc. **6**, 84 (1961).
[9]G. Weber, in *Fluorescence Techniques in Cell Biology*, edited by A. A. Thaer and M. Sernetz (Springer, New York, 1973), p. 5.
[10]F. Perrin, J. Phys. Radium **7**, 1 (1936).
[11]B. Witholt and L. Brand, Biochemistry **9**, 1948 (1970).
[12]M. Shinitsky, A.-C. Dianoux, C. Gitler, and G. Weber, Biochemistry **10**, 2106 (1971).
[13]J. R. Lakowicz and J. R. Knutson, Biochemistry **19**, 905 (1980).
[14]G. Weber, J. Chem. Phys. **66**, 4081 (1977).
[15]G. C. Belford, R. L. Belford, and G. Weber, Proc. Natl. Acad. Sci. U.S.A. **69**, 1392 (1972).
[16]T.-J. Chuang and K. B. Eisenthal, J. Chem. Phys. **57**, 5094 (1972).
[17]M. Ehrenberg and R. Rigler, Chem. Phys. Lett. **14**, 539 (1972).
[18]E. W. Small and I. Isenberg, Biopolymers **16**, 1907 (1977).
[19]F. Perrin, J. Phys. Radium **5**, 497 (1934).
[20]W. A. Steele, J. Chem. Phys. **38**, 2404 (1963).
[21]J. T. Hynes, R. Kapral, and M. Weinberg, J. Chem. Phys. **69**, 2725 (1978).
[22]M. Lederer, Anal. Chim. Acta **6**, 267 (1952); V. S. Gupta, S. C. Kraft, and J. S. Samuelson, J. Chromatogr. **26**, 158 (1967).
[23]M. G. Badea and L. Brand, in *Methods in Enzymology*, edited by C. H. W. Hirs and S. N. Timasheff (Academic, New York, 1979), Vol. 61, part H, p. 378.
[24]L. A. Chen, R. E. Dale, S. Roth, and L. Brand, J. Biol. Chem. **252**, 2163 (1977).
[25]P. R. Bevington, *Data Reduction and Error Analysis for the Physical Sciences* (McGraw-Hill, New York, 1969).
[26]A. Grinvald and I. Z. Steinberg, Anal. Biochem. **59**, 583 (1974).
[27]T. G. McLaughlin, Ph.D. thesis, University of California, San Diego, 1972.
[28]L. B. Clark (unpublished data).
[29]V. Zanker and A. Reichel, Adv. Mol. Spectrosc. **2**, 596 (1962).
[30]V. Hymowitz, Ph.D. Thesis, University of California, San Diego, 1975.
[31]A. Gafni, R. L. Modlin, and L. Brand, Biophys. J. **15**, 263 (1975).
[32]A. Jabtoński, Nuovo Cimento **2**, 995 (1955).
[33]A. A. Newman, *Glycerol* (Chemical Rubber, Cleveland, 1968); J. B. Segur, in *Glycerol*, edited by C. S. Miner and N. V. Dalton (Reinhold, New York, 1953).
[34]G. R. Fleming, J. M. Morris, and G. W. Robinson, Chem. Phys. **17**, 91 (1976).
[35]D. P. Miller, R. J. Robbins, and A. H. Zewail, Proc. Natl. Acad. Sci. U.S.A. **77**, 5593 (1980).
[36]K. G. Spears and L. E. Cramer, Chem. Phys. **30**, 1 (1978).
[37]A. Jabtoński, Z. Naturforsch. Teil A **16**, 1 (1961).
[38]J. Yguerabide, H. F. Epstein, and L. Stryer, J. Mol. Biol. **51**, 573 (1970).
[39]I. Monroe, I. Pecht, and L. Stryer, Proc. Natl. Acad. Sci. U.S.A. **76**, 55 (1979).
[40]P. Wahl, Chem. Phys. **7**, 210 (1975).
[41]G. Lipari and A. Szabo, Biophys. J. **30**, 489 (1980).
[42]D. M. Donaldson, J. M. Robertson, and J. G. White, Proc. R. Soc. London Ser. A **220**, 311 (1953).
[43]A. Heiss, F. Dörr, and I. Kuhn, Ber. Bunsenges. Phys. Chem. **79**, 294 (1975).
[44]R. K. Bauer, H. Grudzinski, A. Jabtoński, and E. Lisicki, Acta Phys. Pol. 33, 803 (1968).
[45]R. K. Bauer and A. Balter, J. Lumin. 20, 249 (1979).

Downloaded 01 May 2008 to 150.131.77.142. Redistribution subject to AIP license or copyright; see http://jcp.aip.org/jcp/copyright.jsp